Superluminal Pulse Propagation in Linear and Nonlinear Photonic Grating Structures

Stefano Longhi, Marcello Marano, Michele Belmonte, and Paolo Laporta

Invited Paper

***Abstract*—Optical pulse propagation in photonic grating structures can show anomalous (i.e., superluminal or negative) group velocities under certain circumstances owing to the anomalous dispersive properties induced by the periodic grating structure. Such phenomena can be observed for either linear pulse propagation in passive dielectric grating structures, such as in fiber Bragg gratings (FBGs), as well as in frequency-conversion processes exploiting second-order cascading effects in quasi-phase-matched (QPM) nonlinear crystals. Engineering of the grating structure can be exploited to observe a wide variety of anomalous pulse transmission and reflection behaviors. In this article, we review the main recent experimental and theoretical achievements obtained by our group in this field. In particular, we report on superluminal propagation of picosecond optical pulses at the 1.5-μm wavelength of optical communications in FBGs, both in transmission and reflection configurations, with the observation of group velocities as large as $\sim 5c_0$. We also show that the phenomenon of transparent pulse propagation at a negative group velocity in a gain doublet atomic amplifier, recently observed in cesium vapor by Wang and co-workers (L. J. Wang, A. Kuzmich, and A. Dogariu, *Nature* vol. 406, pp. 277–279, 2000), can be achieved as well in a photonic parametric amplifier by exploiting the anomalous dispersive properties of the amplifier induced by a suitably designed QPM grating profile.**

***Index Terms*—Anomalous group velocities, Bragg scattering, gratings, optical propagation.**

I. Introduction

THE PROPAGATION of electromagnetic wave packets at a superluminal group velocity has received a renewed interest in the past few years, and a wide series of experiments have to date clearly and unambiguously shown that the group velocity can exceed the speed of light in vacuum or become even negative in suitably prepared physical systems; recent reviews and highlights on this subject are given, e.g., in [1]–[5] and in the present special issue. Though it has been well understood and pointed out by several authors that the observation of anomalous group velocities is compatible with and even a consequence of causality (see, for instance, [5] and references therein), the possibility of speeding up bell-shaped and spectrally narrow optical pulses beyond the speed of light in vacuum remains a rather amazing and counterintuitive phenomenon. The occurrence of anomalous group velocities has been mostly predicted and observed in the framework of two rather distinct physical contexts. One is that of resonant (or near-resonant) pulse propagation through absorbing or amplifying atomic media [6]–[10]; in particular, following the theoretical work by Steinberg and Chiao [8], recently Wang *et al.* [9] have successfully measured negative group velocities of pulse propagation in cesium vapor using stimulated Raman gain under a bichromatic pumping that induces a gain doublet. In this context, the ability to control the optical properties of a medium with a laser field suggests that "fast" and "slow" light propagation effects share common physical features [5]; indeed one can change, in principle, light propagation from subluminal to superluminal by the application of suitable control laser fields [11]. In a completely different context, superluminal group velocities have been considered for a long time in the problem of electromagnetic or matter wave packet tunneling through potential barriers [1], [2]. Superluminal tunneling times have been measured, at either microwave or optical wavelengths, in undersized waveguides [12], [13], periodic dielectric structures [14]–[16], or exploiting frustrated total internal reflection [17]; extended earlier references on this subject can be found, e.g., in [1], [2].

In microwave experiments, superluminal time advancements occur in the nanosecond or picosecond time scale and can be easily revealed using conventional radio-frequency (RF) measurement instruments and techniques. On the contrary, in typical tunneling experimental arrangements using optical probing pulses, such as in optical tunneling through quarter-wave multidielectric mirrors or side-by-side prisms, superluminal peak-pulse advancements fall in the femtosecond time scale and a resolution of a few femtosecond is usually required. Such short events can be detected solely by rather indirect measurements, such as interferometric autocorrelation techniques [16], whereas a direct detection of the signal waveform in the time domain is not possible. The idea of using photonic structures operating at optical wavelengths to either accelerating or slowing down the speed of light, and in particular the use of photonic gratings, photonic band gaps, or high-index photonic structures, is quite recent [18]–[23]. We recently showed that fiber Bragg gratings (FBGs) can be successfully employed not only for pulse control in optical communication and ultrafast optoelectronic applications (see, for instance, [24]), but also as photonic barriers to

Manuscript received September 16, 2002; revised November 22, 2002.

S. Longhi, M. Marano, and P. Laporta are with the Dipartimento di Fisica, Istituto Nazionale per la Fisica della Materia, Milan I-20133, Italy (e-mail: longhi@fisi.polimi.it).

M. Belmonte is with Corning-Optical Technologies Italia S.p.A., Milan I-20126, Italy.

Digital Object Identifier 10.1109/JSTQE.2002.807976

observe different anomalous pulse-propagation effects with picosecond pulses at the 1.5-μm wavelength of optical communications. These include tunneling time measurements across single [23] and double [25] barrier FBGs and the superluminal pulse reflection in specially designed grating structures [26]. Though the use of FBG structures to observe superluminal effects is conceptually similar to analogous photonic Bragg barriers, such as multidielectric quarter-wave Bragg mirrors, the weak Bragg scattering provided by the FBG enables the use of long barriers (up to several centimeters), leading to a huge increase of superluminal peak-pulse advancements by 3–4 orders of magnitude as compared with Bragg mirrors [23]. This permits a direct measurement and recording of the pulse waveforms using a fast sampling oscilloscope when periodic (mode-locked) pulse trains are used. In addition, the synthesis and realization of special grating structures, which is possible today thanks to the recent advances in the field of FBG writing technology, enables us to tailor the dispersive properties of the structure to a high degree of complexity, making it possible to observe in photonic grating structures anomalous pulse-propagation effects similar to those found, e.g., in resonant pulse propagation through atomic systems. For instance, the dispersive properties of a grating structure with two closely spaced resonance modes have been used to observe superluminal reflection of picosecond pulses in [26].

As compared to superluminal effects that can be observed when a pulse propagates through an atomic medium whose dispersive (and absorptive) properties are controlled by a laser field, the use of passive photonic grating structures presents several limitations, that can be summarized as follows. First of all, the tunneling process of pulses through the passive grating structure always leads to strong attenuation due to evanescent wave propagation, so that distortionless "transparent" pulse propagation is not possible using passive photonic structures. Moreover, the achievement of negative group velocities seems unlikely in such structures; indeed, previous experiments on tunneling time measurements have always reported superluminal transit times but never negative ones. Finally, there is not an easy way to control or change the dispersive properties of the structure once it has been designed and realized, using some kind of control field as in atomic systems with electromagnetically controlled optical properties (see, e.g., [11]). Most of these limitations can, nevertheless, be overcome considering pulse propagation in nonlinear grating structures, in which the dispersive properties experienced by a probing optical pulse are strongly influenced by a nonlinear wave interaction process inside a nonlinear crystal and can be changed by use of a control (pump) laser field. In fact, we have recently shown that cascading second-order nonlinear processes may strongly influence the dispersive properties of a probing optical pulse, leading to abnormal group velocities [27]. In particular, we have theoretically shown that in a quasi-phase-matched (QPM) optical parametric amplifier with a suitably designed grating structure, the group velocity of a propagating optical pulse can be controlled by the pump wave and pushed from subluminal to superluminal and negative values by increasing the pump power level [27], [28]. It is remarkable that such an amplifier reproduces the experimental conditions of the gain-assisted superluminal pulse propagation reported by Wang and co-workers [9]. The propagation of optical pulses in nonlinear grating structures, thus, permits to bridge the two different and apparently separated contexts in which superluminal effects are usually encountered.

In this paper, we provide a brief review of the main experimental and theoretical results obtained by our group in the field of superluminal pulse propagation of picosecond optical pulses in photonic grating structures. In Section II, we report on the experimental measurements of tunneling times of picosecond optical pulses at the 1.5-μm wavelength of optical communications using FBGs as photonic barriers. In particular, we present results on tunneling time measurements for single and double barrier (DB) FBGs, providing an experimental evidence in the optical context of the Hartman effect of particle tunneling in quantum mechanics [29], [30]. In Section III, we address the issue of superluminal pulse reflection in asymmetric grating structures, and we demonstrate superluminal reflection of picosecond pulses using a double-Lorentzian (DL) FBG. Section IV is devoted to the analysis of the dispersive properties hidden in pulse propagation through a second-order QPM nonlinear optical parametric amplifier, and the issue of group velocity control in such a device is addressed. Design criteria, based on a periodically poled lithium niobate (PPLN) grating structure, are also given for an experimental observation of negative group velocities at 1.5-μm wavelength. Finally, in Section V the main conclusions are outlined.

II. Tunneling of Picosecond Pulses Through FBGs

This section is devoted to the discussion of the theoretical and experimental results on superluminal propagation of picosecond pulses at 1.5 μm through FBG structures. In particular, we performed experiments on tunneling of pulses through periodic (i.e., uniform) FBGs and through DB structures. When the transmission scheme is adopted, the velocity-of-flight to cross the structure can be estimated from measurements of the tunneling time. After a brief introduction on the theoretical model adopted for light propagation in FBGs, we will present an account of the experimental measurements of tunneling times, both for single periodic barriers [23] and for DB structures [25]. Velocities as large as $\sim 5c_0$ were obtained, in particular, in the latter case, where c_0 is the speed of light in vacuum.

FBGs are optical fiber devices in which the refractive index of the core is modulated along the longitudinal axis, with an almost sinusoidal profile of submicrometric period. This modulation of the refractive index is induced by photorefractive effect exposing the fiber core to an ultraviolet beam, generated from a frequency-doubled Ar-ion laser or from an excimer laser. The periodic intensity profile of the laser beam is typically achieved by the interference pattern from a phase mask. The effective index of a grating is defined as the spatial average of refractive index on the transverse section of the fiber, weighted with the transverse intensity profile of the fiber mode. The effective index profile along the longitudinal axis z can be written as $n(z) = n_0 \{1 + 2h(z)\cos[2\pi z/\Lambda_0 + \phi(z)]\}$ for $0 < z < L$, where Λ_0 is the nominal period of the grating, n_0 is the average effective index, and $h(z)$, $\phi(z)$ describe the slow variation, as

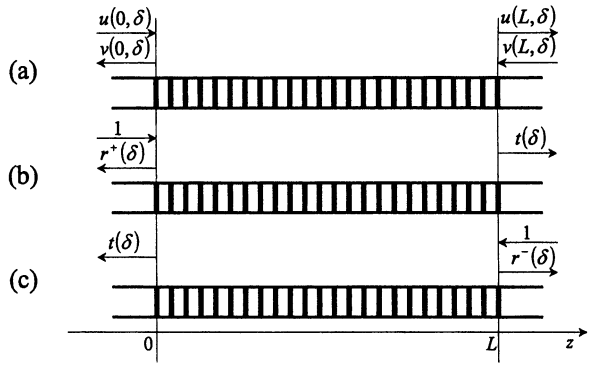

Fig. 1. (a) Schematic of Bragg scattering in an FBG with counterpropagating waves. (b) and (c) Boundary conditions for the calculation of spectral coefficients r^+, r^-, and t for forward and backward incidence.

compared to the scale of Λ_0, of amplitude and phase, respectively, of the index modulation. The periodic modulation of the refractive index along the longitudinal axis of the fiber leads to Bragg scattering between the counterpropagating waves at the same angular frequency ω, provided that this frequency matches the Bragg condition $\omega = c_0\pi/(n_0\Lambda_0)$ [31]. This is the main physical effect that determines the spectral response of a grating structure. The spectral features of an FBG, such as the existence of a frequency stopband, are thus analogous to those generally found in other periodic photonic structures (see, for instance, [31]).

To go deeply into the subject, let us consider a monochromatic field at frequency ω close to the Bragg frequency $\omega_B = c_0\pi/(n_0\Lambda_0)$ propagating along the FBG. The electric field can be written as $E(z,t) = u(z)\exp(-i\omega t + ik_Bz) + v(z)\exp(-i\omega t - ik_Bz)$ + c.c, where u and v are the envelopes of the two counterpropagating waves, $k_B = \pi/\Lambda_0$ is the Bragg wavenumber, and c.c. stands for complex conjugate. It is well known that the slowly varying envelopes u and v, for a weak grating depth ($|h(z)| \ll 1$), satisfy the following coupled-mode equations (see, e.g., [32]):

$$\frac{d}{dz}u(z,\delta) = +i\delta u(z,\delta) + iq(z)v(z,\delta) \tag{1}$$

$$\frac{d}{dz}v(z,\delta) = -i\delta v(z,\delta) - iq^*(z)u(z,\delta). \tag{2}$$

In (1) and (2), $q(z) \equiv k_Bh(z)\exp[i\phi(z)]$ represents the complex-valued scattering potential, whereas $\delta \equiv k_0 - k_B = n_0(\omega - \omega_B)/c_0$ is the detuning parameter between the wavenumber $k_0 \equiv n_0\omega/c_0$ of counterpropagating waves and the Bragg wavenumber k_B. The field envelopes u and v at the $z = 0$ and $z = L$ planes of the grating structure [see Fig. 1(a)], because of the linearity of (1) and (2), are related by the following matrix equation:

$$\begin{bmatrix} u(L,\delta) \\ v(L,\delta) \end{bmatrix} = \mathcal{M}(\delta)\begin{bmatrix} u(0,\delta) \\ v(0,\delta) \end{bmatrix}. \tag{3}$$

The elements of the 2×2 transfer matrix $\mathcal{M}$ satisfy the conditions $\mathcal{M}_{22} = \mathcal{M}_{11}^*$, $\mathcal{M}_{21} = \mathcal{M}_{12}^*$, and $\det\mathcal{M} = 1$. When a single monochromatic light beam is launched into the FBG, there are a reflected and a transmitted beam, whose amplitudes can be calculated by solving (1) and (2) with the appropriate boundary conditions. For a forward-propagating incident beam $z = 0$ and $z = L$ are the input and output planes, respectively, and the boundary condition is $v(L,\delta) = 0$ [see Fig. 1(b)]. The spectral reflection coefficient for forward light incidence is defined by

$$r^+(\delta) = \left[\frac{v(0,\delta)}{u(0,\delta)}\right]_{v(L,\delta)=0} = -\frac{\mathcal{M}_{21}}{\mathcal{M}_{22}}. \tag{4}$$

For a backward-propagating incident beam the light comes from the right side of the grating and the boundary condition is $u(0,\delta) = 0$. Notice that in this case input and output planes are reversed, as illustrated in Fig. 1(c). The corresponding reflection coefficient is, therefore, $r^-(\delta) \equiv [u(L,\delta)/v(L,\delta)]_{u(0,\delta)=0} = \mathcal{M}_{12}/\mathcal{M}_{22}$. The forward reflection coefficient $r^+(\delta)$ is the more commonly used, and in the following we will indicate it by $r(\delta)$ for the sake of simplicity. The spectral transmission coefficient, conversely, is independent of the incidence side [see Fig. 1(b) and (c)] and is given by $t(\delta) = [u(L,\delta)/u(0,\delta)]_{v(L,\delta)=0} = [v(0,\delta)/v(L,\delta)]_{u(0,\delta)=0} = 1/\mathcal{M}_{22}$.

Besides the spectral shape $|t(\delta)|$, an important role is played by the group delay in transmission $\tau_g^{(t)}$, also called the phase time, equal to the first derivative of the phase Φ_t of the transmission coefficient against ω: $\tau_g^{(t)}(\omega) = d\Phi_t/d\omega = (n_0/c_0)d\Phi_t/d\delta$. For an incident pulse with carrier frequency ω_0 and narrow bandwidth, the tunneling time needed to cross the grating structure can be assumed equal to the group delay $\tau_g^{(t)}$ of the grating, evaluated at frequency ω_0 (see, e.g., [33]). The superluminal or subluminal propagation for a pulse transmitted throughout the FBG, therefore, depends on this parameter. Superluminal peak advancement in transmission, for a structure of length L, occurs whenever $\tau_g^{(t)} < L/c_0$. We stress that the group delay provides an accurate estimate of the time delay of the peak-pulse intensity solely for a spectrally narrow optical pulse with a smooth envelope [1], and that superluminal phenomena may be observed only in this case [1], [34], [35]. In fact, the properties of analyticity of the coupled-mode equations ensure that the front of any discontinuous signal may not propagate through the grating at a speed higher than c_0/n_0, i.e., no genuine violation of Einstein causality occurs [1], [34]–[36]. It should also be pointed out that the coupled-mode equations model [(1) and (2)] does not include material dispersion of the fiber; if dispersion were accounted for, $n_0 \to 1$ and $q \to 0$ as $\omega \to \infty$. The front velocity of a discontinuous step-like signal, so, actually travels at the speed of light in vacuum c_0.

For optical communications purposes, FBGs are typically used as linear filters in reflection, because the Bragg scattering mechanism provides a bandpass reflection spectrum; when used in transmission, conversely, they act as band-stop Fourier filters. We will see that superluminal pulse propagation in transmission can occur when the optical spectrum of the incoming pulse is located just in the stopband of the grating.

A. Single Barrier

The reflection and transmission coefficients of an FBG, in general, depend on amplitude and phase profiles of the grating.

The simplest grating is the uniform or periodic FBG, in which $h(z) = h_0$ and $\phi(z) = \phi_0$ are constant along the fiber and, therefore, the scattering potential $q(z) = q_0 \equiv k_B h_0 \exp[i\phi_0]$ is also constant. This structure represents the simplest photonic barrier that can be used to achieve larger-than-c_0 group velocities, for an incident beam with an optical frequency in the spectral region corresponding to the band gap of the grating. In this case, (1) and (2) can be analytically solved, yielding

$$\mathcal{M} = \begin{bmatrix} \cosh(\xi L) + i\frac{\delta}{\xi}\sinh(\xi L) & i\frac{q_0}{\xi}\sinh(\xi L) \\ -i\frac{q_0^*}{\xi}\sinh(\xi L) & \cosh(\xi L) - i\frac{\delta}{\xi}\sinh(\xi L) \end{bmatrix} \tag{5}$$

where $\xi \equiv (|q_0|^2 - \delta^2)^{1/2}$. The reflection and transmission coefficients are, therefore

$$r(\delta) = \frac{iq_0^* \sinh(\xi L)}{\xi\cosh(\xi L) - i\delta\sinh(\xi L)} \tag{6}$$

$$t(\delta) = \frac{\xi}{\xi\cosh(\xi L) - i\delta\sinh(\xi L)}. \tag{7}$$

From (6) it follows that the power spectral reflectivity $R = |r|^2$ is maximum at Bragg resonance, i.e., for $\delta = 0$, and it is equal to $R_{\max} = \tanh^2(|q_0|L)$. Note that $R_{\max}$ approaches 1 for $q_0 L \gg 1$, i.e., for either a sufficiently long grating or for a large modulation depth. The reflectivity bandwidth corresponds approximately to the frequency range in which the parameter ξ is real, i.e., for $|\delta| \le |q_0|$. This means that the spectral bandwidth of a grating is mainly determined by the modulation depth, not by the grating length. By suitably changing the length L and the strength h_0 of the grating, one can achieve the desired peak reflectivity and bandwidth. From (7), we obtain the following expression for the group delay in transmission:

$$\tau_g^{(t)}(\delta) = \frac{n_0 L}{c_0}\frac{|q_0|^2}{\xi^2 + \delta^2\tanh^2(\xi L)} \times \left[\frac{\delta^2}{|q_0|^2}\tanh^2(\xi L) + \frac{1}{\xi L}\tanh(\xi L) - \frac{\delta^2}{|q_0|^2}\right]. \tag{8}$$

Both the power spectral transmission $T(\delta) = |t(\delta)|^2$ and the group delay $\tau_g^{(t)}(\delta)$ show a minimum at the center of the band gap, i.e., for $\delta = 0$, where $T(0) = 1/\cosh^2(|q_0|L) = 1 - R_{\max}$ and $\tau_g^{(t)}(0) = (n_0 L/c_0)\tanh(|q_0|L)/(|q_0|L)$. For a fixed grating strength $|q_0|$, the higher the length L, the lower the power transmission $T(0)$ at the gap center. Note that for $L \to \infty$, i.e., for an opaque barrier, the tunneling time approaches $n_0/(c_0|q_0|)$ and becomes independent of the barrier width. This circumstance is the optical analogous of the Hartman effect [29], known in quantum mechanics in the context of tunneling of a particle through a potential barrier (see also [33]). If the incoming pulse has a narrow spectrum centered at $\delta = 0$, therefore, it can cross the barrier and leave the grating attenuated, but without appreciable distortion of its shape, with a group velocity v_g larger than c_0. The group velocity, in fact, can be estimated simply as the ratio between the barrier width L and the tunneling time $\tau_g^{(t)}(0)$, that is

$$v_g(0) \equiv \frac{L}{\tau_g^{(t)}(0)} = \frac{c_0}{n_0}\frac{\tanh^{-1}\sqrt{R_{\max}}}{\sqrt{R_{\max}}}. \tag{9}$$

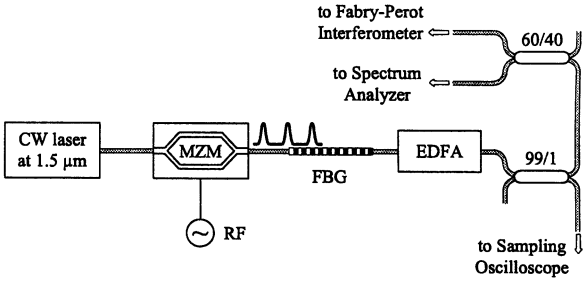

Fig. 2. Schematic of the experimental setup for tunneling experiments in transmission. MZM: Mach–Zehnder waveguide modulator.

A larger-than-c_0 group velocity occurs for a sufficiently opaque barrier such that $\sqrt{R_{\max}} > \tanh(n_0\sqrt{R_{\max}})$. For $n_0 = 1.452$, which is the typical value of the average refractive index for an FBG, this condition becomes $R_{\max} > 70.4\%$. If the spectrum of the incoming pulse, on the contrary, is centered far away from the Bragg frequency of the grating, Bragg scattering does not occur, the pulse travels with a group velocity c_0/n_0 and is not attenuated at the output.

We performed tunneling experiments of picosecond pulses through periodic gratings of different length, i.e., barrier thickness, but designed to have the same Bragg frequency and the same modulation depth h_0, and so comparable bandwidth [23]. The chosen value of the modulation depth was $h_0 = 2.345 \times 10^{-5}$, corresponding to an approximate grating bandwidth $\Delta\nu = 2h_0\omega_B/(2\pi) \sim 10$ GHz, for a carrier frequency in the 1.5-μm wavelength range. The FBGs were fabricated from a deuterium-loaded fiber using a standard writing technique, in which an ultraviolet beam generated by a frequency-doubled Ar-ion laser is focused on a phase mask and strobed using an acoustooptic modulator. The average effective index is $n_0 = 1.452$ for all the gratings. A schematic diagram of the experimental setup is shown in Fig. 2. The probing pulses were generated using a stabilized continuous-wave (CW) Er–Yb:glass laser, externally modulated at a repetition frequency $f_m = 1$ GHz by means of a fiber-coupled $LiNbO_3$ Mach–Zehnder modulator. The laser cavity, similar to that reported in [37], is a one-folded 18-cm-long resonator, in which the active disk is end-pumped at 980 nm by an InGaAs laser diode. An intracavity BK-7 uncoated etalon, with 100-μm thickness, allows for a tuning of the emission laser wavelength by a few nanometers near 1533 nm. A finer tuning (<800 MHz) of the laser frequency, when necessary, is achieved by a submicrometric control of the laser cavity length using a piezoelectric transducer mounted on the output laser mirror.

The Mach–Zehnder modulator was sinusoidally driven at a frequency f_m by an RF synthesizer. For a waveguide modulator with chirp compensation, as the one used for our experiments, the frequency chirping introduced by the modulator is negligible and the electric field E at the output of the modulator is given by

$$E(t) = E_0\cos[\delta_0 + \delta_m\sin(2\pi f_m t)]\exp(i\omega_0 t) \tag{10}$$

where E_0 is the amplitude of the electric field at the input of waveguide, ω_0 is the carrier frequency of the laser, δ_0 is the bias point, and δ_m the modulation depth impressed to the mod-

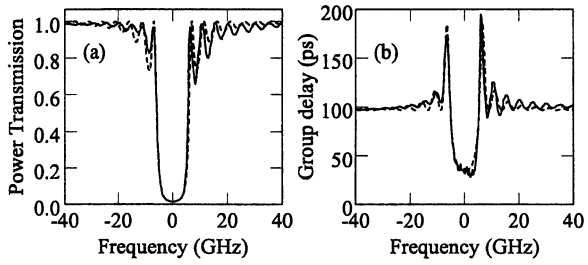

Fig. 3. (a) Spectral power transmission and (b) group-delay for the periodic 2-cm-long FBG used in the experiment. Solid and dashed lines refer to measured and predicted spectral curves, respectively.

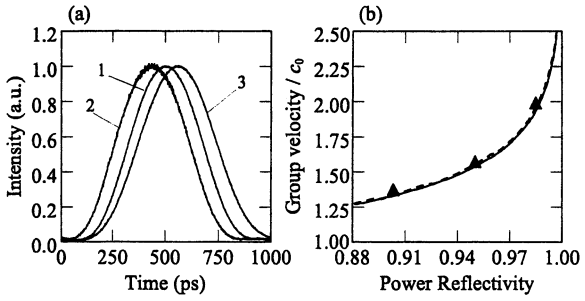

Fig. 4. (a) Pulse traces corresponding to OFF-resonance (curve 1) and ON-resonance (curve 2) propagation. Curve 3 is the pulse trace measured when the pulse spectrum is tuned close to the right-side band gap edge of the FBG. (b) Behavior of group velocity $v_g(0)$ for barrier crossing, normalized to the speed of light in vacuum c_0, as a function of power reflectivity at bandgap center $R_{\max}$, for a uniform FBG with average index $n_0 = 1.452$. The solid curve is obtained by the phase-time analysis [see (9)]. The dashed curve is the theoretical behavior as predicted by numerical propagation of pulse train (10). Triangles refer to measured traversal velocities for three FBGs.

ulator by the sinusoidal RF signal. Proper selection of bias point δ_0 and modulation depth δ_m permits the generation of a pulse train with different pulse durations and pulse shapes. In our case, the bias voltage and the RF level were typically chosen to give $\delta_0 \sim 0.74\pi/2$ and $\delta_m \sim 0.29\pi/2$. With these parameters, the output beam is a pulse train with a full-width at half-maximum (FWHM) pulse duration of ~380 ps and 1-ns periodicity. The chosen pulse shape and duration correspond to a spectral pulse bandwidth of ~2 GHz, that is, about one fifth as compared to the grating bandgap.

After propagation trough the FBG, the transmitted pulse train was sent to a low-noise erbium-doped fiber amplifier (EDFA), with a saturation power of ~30 μW, to keep the power of the transmitted beam at a comparable level (~18 mW) when the laser emission is tuned either inside or outside the bandgap of the grating. The characterization of the transmitted pulse train was performed in the spectral domain using both a scanning Fabry–Pérot interferometer (Burleigh, Mod. RC1101R) with a finesse of ~90, set for a free spectral range of ~27 GHz, and an optical spectrum analyzer (OSA) with 0.07-nm resolution (Anritsu, Mod. MS9710B). In order to carry out a characterization in the time domain simultaneously, the fiber-coupled beam was split, and a small fraction (1%) of the available power was sent to a sampling oscilloscope (Agilent, Mod. 86 100A), triggered by the same low-noise sinusoidal RF signal driving the Mach–Zehnder modulator, thus providing a precise synchronism among successive pulses in the train. The resulting sensitivity of this apparatus for time-delay measurements is of the order of 1 ps.

The first periodic FBG designed and fabricated for the tunneling experiments has a length of $L = 2\,\mathrm{cm}$, corresponding to a minimum power transmission of $T(0) \sim 1.5\%$ at the gap center, as calculated from (7) with $h_0 = 2.345 \times 10^{-5}$. The Bragg frequency of this grating is $\omega_B = 2\pi \times 1.956 \times 10^{14}$ rad/s, i.e., the central wavelength (in vacuum) of the reflectivity spectrum is $\lambda_B = 1533.8$ nm. Fig. 3 shows the theoretically expected (dashed lines) and measured (solid lines) curves for power transmission T and group delay in transmission $\tau_g^{(t)}$ versus frequency detuning $(\omega - \omega_B)/(2\pi)$ for this grating. The group delay was measured using a modulation phase-shift technique [38], [39] which is the more commonly used method for the characterization of FBGs.

We recorded the trace of pulses transmitted through the FBG, as measured by the sampling oscilloscope, for different wavelength tuning conditions of the Er–Yb laser. The absolute value of the carrier wavelength was monitored using the OSA, and its exact position relative to the Bragg wavelength was monitored using the Fabry–Pérot interferometer, previously used to record the reflectivity spectrum of the grating with a high resolution. The pulse spectrum was first detuned far away from the Bragg wavelength of the grating by ~120 GHz, and the transmitted pulse train is shown in Fig. 4(a), trace 1. In this case, the Bragg scattering inside the grating is negligible, and thus, the pulse travels across the barrier with a velocity equal to c_0/n_0. We then tuned the laser spectrum close to the center of the bandgap and we recorded the trace of transmitted pulse, which is shown in Fig. 4(a), trace 2. A temporal advancement of the transmitted pulse peak of ~63 ps, as compared to that of trace 1, can be clearly observed; note that there is no appreciable pulse distortion. The measured pulse advancement corresponds to a velocity for barrier crossing equal to $\sim 1.97c_0$, very close to the theoretical value $v_g(0) \sim 1.94c_0$, calculated from (9) with $R_{\max} = 98.5\%$. We checked that the observed superluminal tunneling time is easily reproducible and persists by changing the operational conditions of the Mach–Zehnder modulator, i.e., pulse duration and modulation frequency. Finally, the carrier wavelength was detuned apart from the bandgap center by ~7 GHz, i.e., close to the first side peak of transmission curve at the bandgap edge. In this case, the behavior of group delay, as shown in Fig. 3(b), indicates a peak-pulse delay, as compared to OFF-resonance propagation, of ~65 ps, i.e., pulse slowing down occurs for such a tuning condition. The pulse trace measured in this case, shown in Fig. 4(a), trace 3, clearly demonstrates pulse slowing down with a pulse-peak delay of ~60 ps, close to the expected value. A slight pulse distortion can be appreciated in this case, which is ascribable to spectral pulse reshaping produced by grating band edge effects.

We also designed and fabricated two other FBGs, with the same Bragg frequency and modulation depth, but with different length, namely 1.6 and 1.3 cm. The gratings were characterized and then used to perform tunneling experiments at different group velocities. According to (9), in fact, the group velocity at the bandgap center is a function of the peak power reflectivity $R_{\max}$ solely, which in turns depends on the barrier thickness L

TABLE I
ANALOGIES BETWEEN TUNNELING OF OPTICAL WAVES AND ELECTRONS IN A SYMMETRIC RECTANGULAR DB POTENTIAL

Photons	Electrons
Equations	
$du/dz = i\delta u + iq(z)v$	$\frac{d^2\psi}{dz^2} + \frac{2m}{\hbar^2}[E - V(z)]\psi = 0$
$dv/dz = -i\delta v - iq^*(z)u$	
DB Transmission[a] (off-resonance)	
$T(\delta = 0) = 1/\cosh^2(2\lvert q_0\rvert L)$	$T(E = V_0/2) = 1/\cosh^2(2\chi L)$
Phase time[a] (off-resonance)	
$\tau = \mathrm{Im}\left\{\frac{\partial \ln(t)}{\partial \omega}\right\} = \tau_1 + \tau_2$	$\tau = \hbar\ \mathrm{Im}\left\{\frac{\partial \ln(t)}{\partial E}\right\} = \tau_1 + \tau_2$
$\tau_1 = [n_0/(c_0\lvert q_0\rvert)]\tanh(2\lvert q_0\rvert L)$	$\tau_1 = [2/(\chi v_g)]\tanh(2\chi L)$
$\tau_2 = (n_0 d/c_0)/\cosh(2\lvert q_0\rvert L)$	$\tau_2 = (d/v_g)/\cosh(2\chi L)$

[a]For electrons, calculations are made assuming a mean-energy of incident wavepacket equal to half of the barrier height, i.e., $E = V_0/2$, and assuming OFF-resonance tunneling, i.e., χL is an integer multiple of $\pi/2$, where $\chi \equiv \sqrt{mV_0}/\hbar$ is the wavenumber of the oscillatory wavefunction between the two barriers. $v_g \equiv \hbar\chi/m$ is the group velocity of free wavepacket.

and on the grating strength $|q_0|$. The experimental results, corresponding to the three FBGs with lengths of 1.3, 1.6, and 2 cm, are shown in Fig. 4(b), together with the theoretical curves obtained either by phase-time analysis [see (9)] or by numerical propagation of the pulse train (10) through the FBG, using the spectral transmission function given by (7).

B. Double Barrier

Besides superluminal propagation and the Hartman effect observed in periodic FBGs, tunneling through DB photonic structures shows even a more amazing phenomenon, namely the independence of the transit time not only of barrier width, but also of barrier separation (generalized Hartman effect [30]). Here, we report our results recently obtained in the measurement of tunneling delay times in DB photonic structures based on FBG technology [25]. Our results represent an extension at optical wavelengths of similar experimental achievements previously reported at microwaves [12], [15], [40], [41] and provide a clear experimental evidence that, for opaque barriers, the traversal time is independent of barrier distance. After a brief account on the quantum-mechanical analogy of electron tunneling and on the basic model of tunneling in a DB rectangular FBG (see also [25]), the main experimental results are presented.

The DB designed and manufactured for the tunneling time measurements at 1.5 μm consists of a single-mode optical fiber in which two periodic Bragg gratings, separated by a distance d, are sequentially written onto it. Each grating has a length L, so that the structure shows an amplitude profile $h(z)$ that simulates a symmetric rectangular DB structure, i.e., $h(z) = h_0$ constant for $0 < z < L$ and $d + L < z < d + 2L$, and $h(z) = 0$, otherwise. For such a structure, Bragg scattering of counterpropagating waves at a frequency ω close to the Bragg resonance $\omega_B = c_0\pi/(n_0\Lambda_0)$ occurs in the grating regions, whereas multiple wave interference between the two barriers leads to Fabry–Pérot resonances in the transmission spectrum. The problem of tunneling through a DB FBG structure bears a close connection to that of nonrelativistic electrons through a symmetric rectangular DB potential, which has been widely investigated in literature (see, for instance, [30], [42]). The analogy between tunneling of electrons and photons in superlattice structures and closed-form solutions for the tunneling times have been recently reported, in the general case, in [43]. The derivation here presented of photon tunneling times follows a different and simpler approach, based on the coupled-mode equations model, which is suited in particular for FBG structures. The analogy with electron tunneling through a rectangular double potential barrier is summarized in Table I, where the basic equations and the expressions of power transmission and group delay are given in the two cases [25], [44]. The electronic potential $V(z)$ is assumed to be $V(z) = V_0$ constant for $0 < z < L$ and $d + L < z < d + 2L$, and $V(z) = 0$, otherwise.

In the electromagnetic case, the counterpropagating waves are oscillatory (propagative) in the region $L < z < d + L$, whereas they are exponential (evanescent) inside the gratings when $|\delta| < |q_0|$. The spectral transmission $t(\omega)$ of the structure can be analytically determined by extending the transfer matrix analysis presented in Section II-A (see also [45]). As an estimate of the tunneling time for a wavepacket crossing the structure, we use again the group delay, which, following a different but equivalent expression to that previously adopted, is given by $\tau_g^{(t)}(\omega) = \mathrm{Im}\{\partial \ln t/\partial\omega\}$. Far from the sharp Fabry–Pérot resonances, the group delay is shorter than that for free propagation from input to output planes, and thus, superluminal propagation occurs for a spectrally narrow incoming pulse. Near the Fabry–Pérot resonances, on the contrary, light slowing down is attained, as in a usual Fabry–Pérot resonator (resonant tunneling). At the center of the bandgap ($\delta = 0$), simple analytical expressions for the power transmission and group delay can be derived and read

$$T(0) = \frac{1}{\cosh^2(2|q_0|L)} \tag{11}$$

$$\tau_g^{(t)}(0) = \tau_1 + \tau_2 \tag{12}$$

where

$$\tau_1 = \frac{n_0}{c_0|q_0|}\tanh(2|q_0|L) = \sqrt{1 - T(0)}\frac{n_0}{c_0|q_0|} \tag{13}$$

$$\tau_2 = \frac{n_0 d}{c_0}\frac{1}{\cosh(2|q_0|L)} = \sqrt{T(0)}\frac{n_0 d}{c_0}. \tag{14}$$

Equations (12)–(14) clearly show that two distinct contributions are involved in the expression for the group delay. The former term τ_1 is independent of the barrier separation, and coincides with the tunneling time of a *single* barrier of width $2L$. As we previously observed, for an opaque barrier ($2|q_0|L \gg 1$) τ_1 becomes independent of barrier width and saturates to the value $n_0/(c_0|q_0|)$ (Hartman effect). Conversely, the latter contribution τ_2 is always shorter than the free-propagation time over a length d and tends to zero for an opaque barrier, implying that the tunneling time becomes independent of barrier distance (*generalized* Hartman effect). Similar results can be obtained for OFF-resonance tunneling of a nonrelativistic electron through a rectangular DB potential $V(z)$ assuming that the incident wavepacket has a below-barrier mean energy E equal to half the barrier width V_0. The corresponding expressions for barrier transmission and group delay in this case are given in Table I. The tunneling through a DB FBG structure can hence be

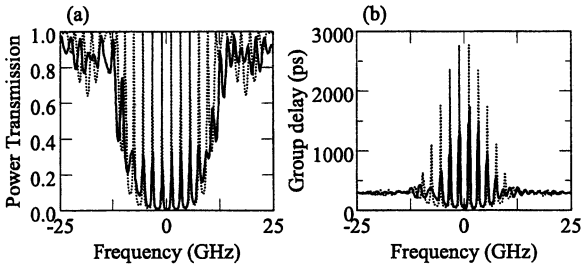

Fig. 5. (a) Spectral power transmission and (b) group delay for a DB FBG structure with $L = 8.5$ mm, $d = 42$ mm, $h_0 = 3.1 \times 10^{-5}$, and $n_0 = 1.452$. Solid and dotted lines refer to measured and predicted spectral curves, respectively.

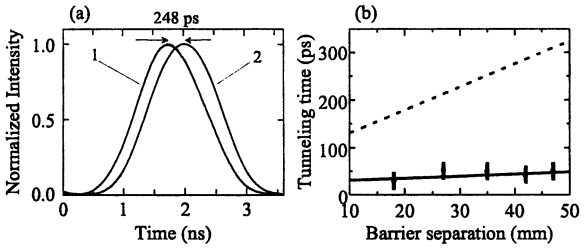

Fig. 6. (a) Temporal intensity profiles corresponding to the pulses transmitted through the DB FBG with 42-mm separation for OFF-resonance tunneling (curve 1) and reference pulse propagating outside the stopband of the structure (curve 2). (b)OFF-resonance tunneling time versus barrier separation L for a rectangular symmetric DB FBG structure. The solid line is the theoretical prediction based on group delay calculations [see (12)–(14)]. Dots are the experimental points as obtained by time-delay measurements. The dashed curve is the transit time from input ($z = 0$) to output ($z = 2L + d$) planes for a pulse tuned far away from the stopband of the FBGs.

used as an experimental verifiable model for the quantum-mechanical case.

To assess the independence of the peak-pulse transit times with barrier distance d, we fabricated five different DB structures with grating spacing d =18, 27, 35, 42, and 47 mm, and we performed tunneling time measurements similar to the single-barrier experiments described in Section II-A. In each structure, the two gratings have sharp fall-off edges, length $L \simeq 8.5$ mm and index modulation depth $h_0 \simeq 3.1 \times 10^{-5}$. The resulting power transmission at antiresonance for the DB structures is $T(0) \simeq 0.8\%$ in all cases, which is low enough to get the opaque barrier limit but yet large enough to perform time-delay measurements at reasonable power levels. The Bragg resonance was set near 1550-nm wavelength. For such structures, both transmission spectra and group delays were measured using a phase-shift technique [38], [39] with a spectral resolution of $\simeq$ 2 pm. As an example, the measured spectral transmission and group delay curves versus frequency detuning of the DB FBG with $d = 42$ mm are shown in Fig. 5. Note that the sharp Fabry–Pérot resonances are not fully resolved in the experimental curves because of the resolution limit of the measurement apparatus ($\sim$2 pm). The expected time advancements in the superluminal spectral regions, far from the Fabry–Pérot resonances, are of the order of 240–250 ps according to the theoretical curve shown in the same figure. Since both transmission and group delay are slowly varying functions of frequency far from Fabry–Pérot resonances, pulse advancements with weak pulse-shape distortion are expected for OFF-resonance pulse transmission.

Direct time-domain measurements of tunneling delay times were performed in transmission experiments using a 300-MHz repetition-rate pulse train with 1.3-ns pulse duration, generated by the Mach–Zehnder modulator, and thus, with pulse shape described by (10). The repetition-rate and the pulse duration were chosen to obtain a spectral pulse bandwidth ($\sim$600 MHz) which is lower than the frequency spacing between adjacent Fabry–Pérot resonances ($\sim$2 GHz for the case shown in Fig. 5) for all five DB structures. The experimental setup and measurement apparatus is analogous to that previously described for single-barrier tunneling experiments and shown in Fig. 2, except than for the CW laser at 1.5 μm, which in this case is a single-mode tunable semiconductor laser (Santec, Model ECL-200/210), equipped with both a coarse and a fine (thermal) tuning control of frequency emission with a resolution of $\sim$100 MHz. The fiber-coupled 10-mW output power emitted by the laser diode was amplified using a high-power EDFA (IPG, Model EAD-2-PM), and then sent to the Mach–Zehnder modulator. The average power of the pulse train available for the transmission experiments was $\sim$130 mW. The reflectivity spectrum of the DB FBG was first measured by the Fabry–Pérot interferometer, set for a free spectral range of $\simeq$ 50 GHz, and with a measured finesse of $\sim$180, by sending to the DB structure, through a three-port optical circulator, the broad-band amplified-spontaneous emission signal generated by the low-noise EDFA in absence of the input signal. The corresponding trace was recorded on a digital oscilloscope and then used as a reference to tune the pulse spectrum at the center of the OFF-resonance plateau between the two central resonances of the DB structure.

In Fig. 6(a), curve 1 shows a typical measured trace, averaged over 64 acquisitions, of the tunnelled optical pulses under OFF-resonance tuning condition, for the DB FBG with 42-mm separation. The trace measured when the laser was detuned by $\sim$200 GHz, i.e., far away from the stopband of the DB FBG structure, is also shown for comparison in Fig. 6(a), curve 2. The tunnelled pulses are almost undistorted with a peak-pulse advancement of $\simeq$ 248 ps; repeated measurements showed that the measured pulse-peak advancement is accurate within $\pm$15 ps, the main uncertainty in the measure being determined by the achievement of the optimal tuning condition.

Time-delay measurements were repeated for the five DB FBG structures, and the experimental results are summarized in Fig. 6(b) and compared with the theoretical prediction of tunneling time as given by (12)–(14). The dashed line in the figure shows the theoretical transit time versus barrier separation d, from input ($z = 0$) to output ($z = 2L + d$) planes, for pulses tuned far away from the bandgap of the FBG structure. In this case, the transit time is given simply by the time spent by a pulse traveling along the fiber for a distance $2L + d$ with a velocity $c0/n_0$. The solid line is, in turn, the expected transit time for OFF-resonance tunneling of pulses, according to (12)–(14), and shows that the transit time does not substantially increase with the barrier spacing (generalized Hartman effect). The points in the figure were obtained by subtracting to the dashed curve the measured peak-pulse advancements for the five DB FBGs, thus

providing experimental estimates of the tunneling transit times. Note that, within the experimental errors, a rather satisfactory agreement between measured and predicted transit times was achieved. The measured transit times are superluminal for all five DB structures. It is remarkable that, for the longest barrier separation used ($d = 47$ mm), the observed transit time corresponds to a superluminal velocity of about $5c_0$, the largest one measured so far in tunneling experiments at optical wavelengths. We mention that superluminal group velocities as large as $\sim 10c_0$ were previously observed by G. Nimtz and co-workers, but in microwave transmission experiments.

III. Superluminal Pulse Reflection From Asymmetric FBGs

In the analysis of tunneling problems of photons across photonic gratings, a closely related issue is that of the temporal behavior of the reflected wave, which arises from Bragg scattering in the structure. In particular, a major question is whether it is possible for a pulse incident upon an FBG structure to be reflected *in advance* without appreciable distortion, albeit attenuated, from the entrance plane of the structure. This is indeed the case, and such an anomalous behavior of pulse reflection has been considered in few articles. In particular, we have recently shown in [22] and [26] that *asymmetric* Bragg grating structures can be designed and fabricated to observe superluminal effects in pulse reflection. This situation occurs whenever the group delay in reflection $\tau_g^{(r)}$ of the structure, for either one of the two incident sides, is negative within a certain spectral region. The need for a grating with an asymmetric profile for the amplitude and/or the phase of refractive index modulation stems from the analytic properties in the complex plane of transmission and reflection spectral functions of any passive loss-less grating structure, ensured by the principle of causality. These properties, in fact, lead to the following inequality between power spectral reflectivity $R(\delta) \equiv |r(\delta)|^2$ and group delay $\tau_g^{(r)}(\delta)$ at either one side of incidence [22], [46]

$$\tau_g^{(r)}(\delta) \geq -\frac{n_0}{\pi c_0} \int_{-\infty}^{\infty} \frac{\partial \ln \sqrt{R(\delta')}}{\partial \delta'} \frac{d\delta'}{\delta' - \delta} \tag{15}$$

where the equality occurs for an FBG with minimal phase shift. For a symmetric grating structure, one has $\tau_g^{(r)} = \tau_g^{(t)}$ and, since $\tau_g^{(t)}$ is typically positive though superluminal, the reflected peak pulse escapes from the grating after the peak of the incident pulse has entered into the grating region. For an asymmetric grating, one has $\tau_g^{(t)} = \left[\tau_g^{(r+)} + \tau_g^{(r-)}\right]/2$, where the $\pm$ sign indicates the side of incidence [see Fig. 1(b) and (c)], so that one can have, e.g., $\tau_g^{(r+)} < 0$ though $\tau_g^{(t)}$ is positive. In particular, if the FBG has a local minimum of spectral reflectivity $R(\delta')$ at the bandgap center $\delta' = 0$, the integral on the right-hand side in (15) turns out to be positive for δ ranging in a neighborhood of zero, and hence $\tau_g^{(r)}$ is allowed to become negative. A simple method to achieve a minimum of spectral reflectivity at the bandgap center, proposed in [22], consists in introducing in an otherwise uniform periodic grating a defect, such as a π phase slip, in an asymmetric position. A different possibility is to synthesize *ab initio*, using inverse scattering methods, a spectral reflectivity function $r(\delta)$ that provides the desired negative group delay. In particular, we recently proposed and experimentally demonstrated [22], [26] superluminal reflection of picosecond pulses at 1.5 μm from a DL FBG structure. A DL FBG possesses two resonance modes [32] which realize a spectral reflectivity profile given by the interference of two closely spaced complex Lorentzian lines. The dispersion curve *in reflection* realized by a DL FBG is analogous to that produced in an inverted medium with a gain doublet [8], [9] where a negative group-delay *in transmission* is achieved by exploiting the interference of the two Lorentzian lines of the homogeneously broadened atomic transitions.

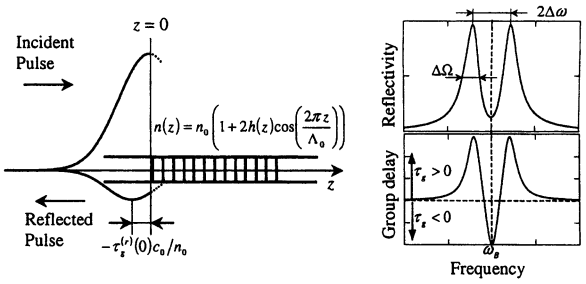

Fig. 7. Principle of superluminal pulse reflection in a DL FBG. When the peak of the incident pulse enters into the grating at input plane $z = 0$, the peak of the reflected pulse has already left the grating in advance and travelled backward the distance $2|\Delta L| = -\tau_g^{(r)}(0)c_0/n_0$. For the sake of clearness, peak advancement and amplitude of the reflected pulse have been exaggerated. Upper and lower pictures on the right-hand side show schematically the spectral power reflectivity and group delay of a DL FBG.

The principle of superluminal pulse reflection in a DL FBG is shown in Fig. 7. The peak of a pulse incident upon the FBG is reflected in advance due to a negative group delay $\tau_g^{(r)}$ which occurs when the pulse spectrum is centered near the Bragg frequency ω_B. The explicit form of the spectral reflectivity in a DL FBG is

$$r(\delta) = \frac{i\kappa}{\delta + \epsilon + i\gamma} + \frac{i\kappa}{\delta - \epsilon + i\gamma} \tag{16}$$

where ϵ, γ, and κ are positive real-valued parameters that determine frequency separation $2\Delta\omega$, width $\Delta\Omega$, and strength of the two Lorentzian lines, respectively (see Fig. 7). The qualitative behavior of power spectral reflectivity $R(\omega)$ and group delay $\tau_g^{(r)}$ is shown in Fig. 7 as well. The minimum of group delay is attained in correspondence of the minimum of spectral reflectivity $R(\omega)$, i.e., at $\omega = \omega_B$, and is given by $\tau_g^{(r)}(0) = n_0(\gamma^2 - \epsilon^2)/[\gamma c_0(\gamma^2 + \epsilon^2)]$. Superluminal peak-pulse advancement in reflection for a pulse tuned close to $\omega = \omega_B$, therefore, occurs for $\epsilon > \gamma$, i.e., when the two Lorentzian lines are sufficiently spaced[1].

The reflectivity profile given by (16) is realized by an unchirped grating with an amplitude modulation profile $h(z)$ which can be determined by simple Fourier transform of (16) for a weak reflectivity. Since the spectral reflectivity is a rational

[1]It should be noted that in case of pulse propagation through an atomic medium with a gain doublet, the spectral transmission function is actually given by the exponential of two closely spaced Lorentzians. Nevertheless, the behavior obtained assuming the Ansatz (16), which makes simpler the grating design, is qualitatively the same. Note also that, adopting our Ansatz, the pulse advancement turns out to be independent of grating strength.

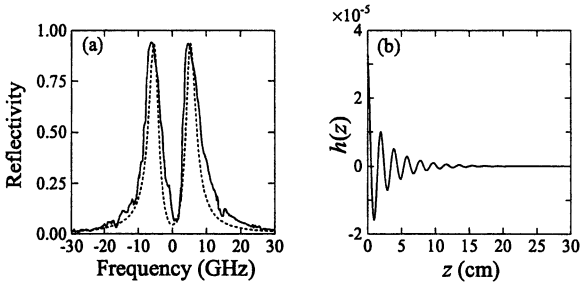

Fig. 8. (a) Measured spectral power reflectivity of the DL FBG used in the experiment (solid line) and corresponding theoretical curve (dashed line). Parameter values are: $n_0 = 1.452$, $\omega_B = 2\pi \times 1.935 \times 10^{14}$ rad/s, $\Delta\omega = 2\pi \times 5.4 \times 10^9$ rad/s, $\epsilon/\gamma = 3$, and $\kappa/\gamma = 0.92$. (b) Amplitude profile $h(z)$ of refractive index for the DL FBG as obtained by the Gel'fand–Levitan–Marchenko inverse scattering method.

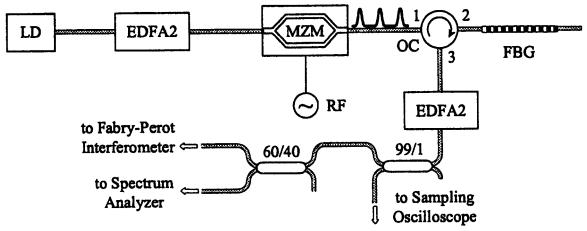

Fig. 9. Schematic of the experimental setup. LD: tunable laser diode; MZM: Mach–Zehnder waveguide modulator; OC: optical circulator.

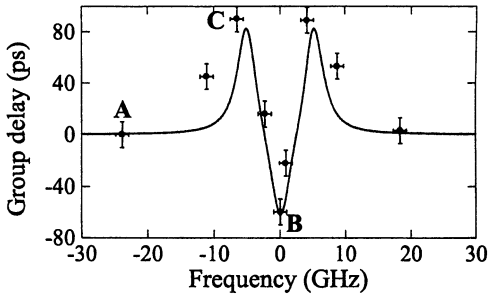

Fig. 10. Measured (circles) and predicted (solid curve) group delay versus frequency detuning from Bragg resonance. In the experimental measurements, the group delay for the red-shifted OFF-resonance pulse (point A in the figure) has been taken equal to zero for reference.

function, an analytical expression of $h(z)$ can be derived even for a high reflectivity using the Gel'fand–Levitan–Marchenko inverse scattering method [22], [32], [47]. In our experiment, we fabricated a 30-cm-long DL FBG by a continuous writing technique with a Bragg resonance at 1550 nm and with a separation of the Lorentzian lines of 10.8 GHz; a negative group delay $\tau_g^{(r)} \sim 62$ ps and power reflectivity $R \sim 5\%$ were obtained at $\omega = \omega_B$. The measured and designed spectral reflectivity profiles of the grating are shown in Fig. 8(a); the amplitude profile $h(z)$ of the corresponding structure is also shown in Fig. 8(b).

Group delay measurements were performed in the time domain analyzing with the fast sampling oscilloscope the reflected beam when a train of optical pulses at 1.5 μm was launched into the DL FBG for different tuning conditions. The experimental setup for time-delay measurements, shown in Fig. 9, is similar to that used in transmission experiments described in Section II, except that now an optical circulator is used to retrieve the pulse train reflected from the Bragg grating (see Fig. 9). The probing pulse train, generated by the external Mach–Zehnder modulator, has a repetition frequency of 1 GHz, and each pulse has a duration (FWHM) of $\simeq$ 380 ps and a spectral extent of $\simeq$ 2 GHz, narrower than the $\simeq$ 4 GHz FWHM of each Lorentzian line.

Fig. 10 shows the measured pulse delays (points) versus frequency detuning, together with the theoretical dispersion curve, assuming the OFF-resonance pulse A in the figure as a reference, i.e., $\tau_g^{(r)} \simeq 0$ for such a pulse [26]. Notice that, close to the two resonance lines of the structure, pulse reflection is subluminal, with a measured peak-pulse delay of $\sim$90 ps, whereas midway of the two resonances superluminal pulse reflection is attained, with a peak-pulse advancement of $\simeq$ 60 ps.

IV. Anomalous Dispersion and Negative Group Velocities in Second-Order Nonlinear Optical Interactions

The tunneling experiments described in Sections II and III that use FBGs as photonic barriers, have allowed us to observe superluminal tunneling times at optical wavelengths in the picosecond time scale with direct time-domain measurements. However, with such passive grating structures, the achievement of negative transit times, corresponding to a transmitted peak pulse that leaves the structure earlier than the peak of the incoming pulse has entered into the grating, seems unlikely. In addition, it would be of some relevance to externally control the group velocity of tunnelled pulses using, e.g., a control laser field as in pulse propagation through atomic media with electromagnetically controlled optical properties. In this section, we show theoretically that, exploiting the dispersive properties of nonlinear optical interactions in second-order QPM gratings, such goals can be achieved. In particular, we show that propagation of a weak signal probe in a suitably designed optical parametric amplifier under strong pumping can exactly reproduce the experimental condition of the gain-assisted transparent pulse propagation experiment by Wang *et al.* [9]. It should be noted that, though nonlinear $\chi^{(2)}$ QPM grating structures have been extensively studied in connection with a great variety of pulse shaping and control functions (see, e.g., [48]–[51]), many dispersive properties hidden in second-order nonlinear optical interactions, especially those related to the occurrence of anomalous group velocities, have not been fully investigated yet. In [27], we recently studied at some general extent the dispersive properties of nondegenerate optical parametric amplifiers based on QPM nonlinear crystals and we derived general relations between the gain and dispersive properties of the amplifier. Here, we briefly review the main results of our analysis on QPM nondegenerate parametric amplifiers, however, we envisage that the issue of group velocity control based on nonlinear frequency conversion and wave mixing processes should be a rather general feature and will be the subject of future investigations[2] [52], [54].

The dispersive properties of a QPM optical parametric amplifier share many common features with those of a linear Bragg

[2]We just mention that the occurrence of superluminal group velocities in nonlinear wave mixing has been considered until now solely in very few papers.

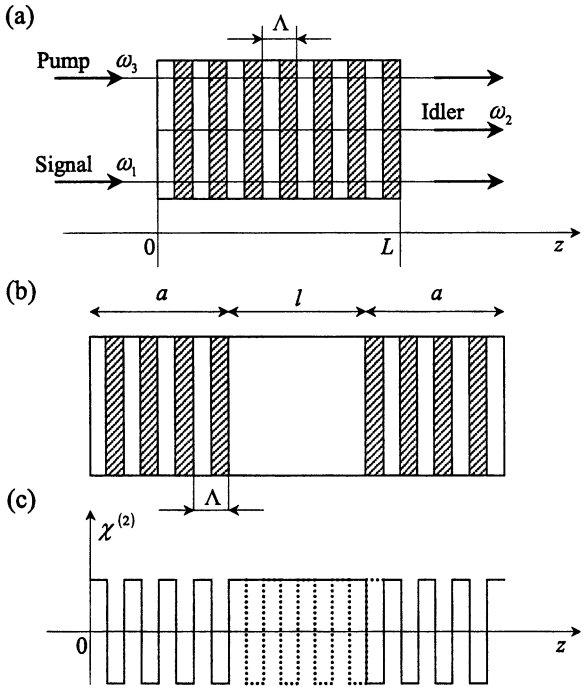

Fig. 11. (a) Parametric amplification of a weak signal wave at frequency ω_1 in a QPM second-order nonlinear crystal of length L pumped by a strong pump wave at frequency ω_3. QPM is accomplished for the generation of the copropagating idler wave at frequency $\omega_2 = \omega_3 - \omega_1$. (b) Schematic of a double QPM grating structure showing negative transit times. Two uniform grating sections, each of length a, are separated by a distance l with no grating structure. (c) QPM square-wave profile of $\chi^{(2)}(z)$ corresponding to a phase shift Φ between the two square waves equal to π.

grating structure, though some basic distinctions appear in the analysis which arise from the basically different physics underlying the wave dispersion mechanisms in the two cases. In the undepleted pump limit, the parametric amplification of a (weak) signal wave at carrier frequency ω_1, pumped by a (strong) pump wave at frequency ω_3, is governed by a set of two linear equations for the signal and the idler wave, at frequency $\omega_2 = \omega_3 - \omega_1$, which is generated in the parametric down-conversion of the pump photons. We assume a linearly polarized plane-wave electric field $E(z,t) = (1/2)[A_1(z,t)\exp(ik_1 z - i\omega_1 t) + A_2(z,t)\exp(ik_2 z - i\omega_2 t) + A_3(z,t)\exp(ik_3 z - i\omega_3 t) + \text{c.c.}]$ propagating along the z axis of a loss-less QPM $\chi^{(2)}$ crystal of length L [see Fig. 11(a)], where A_l $(l = 1,2,3)$ are the slowly varying envelopes of signal, idler, and pump waves, respectively, $k_l = k(\omega_l) = (2\pi/\lambda_l)n_l$ are their wave vectors and n_l the refractive indices at wavelengths λ_l. The resulting coupled equations for the amplitudes A_1 and A_2 are (see, e.g., [27])

$$\frac{\partial A_1}{\partial z} + \frac{1}{v_{g1}}\frac{\partial A_1}{\partial t} = i\frac{\omega_1 d_{\text{eff}}(z)}{n_1 c_0}\frac{2I_3}{(\epsilon_0 c_0 n_3)^{1/2}}A_2^* \qquad (17)$$

$$\frac{\partial A_2}{\partial z} + \frac{1}{v_{g2}}\frac{\partial A_2}{\partial t} = i\frac{\omega_2 d_{\text{eff}}(z)}{n_2 c_0}\frac{2I_3}{(\epsilon_0 c_0 n_3)^{1/2}}A_1^* \qquad (18)$$

where $v_{g1,2} = 1/k'(\omega_{1,2})$ are the group velocities of signal and idler fields, I_3 is the intensity of the pump wave, $d_{\text{eff}}(z) = (1/2)\overline{\chi^{(2)}(z)\exp(i\Delta k z)}$, $\Delta k \equiv k_3 - k_2 - k_1$ is the wave vector mismatch, and the overline denotes a spatial average over the short coherence length $\Lambda = 2\pi/\Delta k$ $(\Lambda \ll L)$. For the sake of simplicity, in writing (17) and (18), we neglected group velocity dispersion and higher order material dispersion terms; the inclusion of these terms, in fact, does not substantially change the results of the analysis [27]. In first-order QPM, the $\chi^{(2)}$ grating is usually obtained by a square-wave $\pm$ reversal of domains in a ferroelectric crystal with a local period (close to Λ) and a local duty cycle that are slowly varying along the z axis. The resulting *slowly varying* profile of the effective nonlinear term $d_{\text{eff}}(z)$ comes from the local changes of period and duty cycle in the *rapidly varying* square-wave grating $\chi^{(2)}(z)$ (see, e.g., [51]). To see the analogy of the parametric (17) and (18) with the coupled-mode (1) and (2), we can perform a spectral analysis of (17) and (18). By setting $A_1(z,t) = [\omega_1/(n_1\omega_3)]^{1/2}u(z,\Omega)\exp[i\Omega(t - z/v_g)]$ and $A_2(z,t) = [\omega_2/(n_2\omega_3)]^{1/2}v^*(z,\Omega)\exp[-i\Omega(t - z/v_g)]$, where Ω is the frequency offset from the carrier frequencies and $v_g \equiv 2v_{g1}v_{g2}/(v_{g1} + v_{g2})$ is a mean group velocity, one obtains indeed for the spectral amplitudes u and v the coupled mode (1) and (2) of passive loss-less grating theory, provided that we set now

$$\delta \equiv \left(\frac{\Omega}{2}\right)\left(\frac{1}{v_{g1}} - \frac{1}{v_{g2}}\right) \qquad (19)$$

for the detuning term, and

$$q(z) \equiv d_{\text{eff}}(z)\left[\frac{8\pi^2 I_3}{(\epsilon_0 c_0 n_1 n_2 n_3 \lambda_1 \lambda_2)}\right]^{1/2} \qquad (20)$$

for the scattering potential. Note that the spectral gain coefficient of the amplifier is given by $g(\Omega) = [u(L,\Omega)/u(0,\Omega)]_{v(0,\Omega)=0}\exp[-i(L/v_g)\Omega]$, and it is thus related to the elements of the transfer matrix $\mathcal{M}$, given in (3), by $g(\Omega) = \mathcal{M}_{11}\exp[-i(L/v_g)\Omega]$. The spectral power gain curve of the amplifier is then given by $G(\Omega) = |g(\Omega)|^2$, whereas the transit time of a signal wave packet spectrally narrow around the frequency Ω_0 is given by the "complex" group delay

$$\Delta\tau = -i\left(\frac{\partial \ln g}{\partial \Omega}\right)_{\Omega_0} = \tau_g(\Omega_0) - i\left(\frac{\partial \ln \sqrt{G}}{\partial \Omega}\right)_{\Omega_0} \qquad (21)$$

where $\tau_g = \partial\phi_g/\partial\Omega$ is the usual real-valued group delay (or phase time) as that appearing in (8), and $\phi_g(\Omega)$ is the phase of $g(\Omega)$ [27]. The imaginary term entering in (21), which accounts for pulse distortion effects at leading order, vanishes when the frequency Ω_0, is tuned in correspondence of a minimum or maximum of the spectral power gain curve, and in such cases can be, hence, disregarded. In what follows, it is important to have in mind that as a consequence of the causality of the coupled-mode (1) and (2), the group delay τ_g is uniquely determined by the spectral power gain curve $G(\Omega)$ through a Hilbert-like transform (see [27]; see also [46]), namely

$$\tau_g(\Omega) = \frac{L}{v_{g1}} \pm \frac{1}{\pi}\int_{-\infty}^{\infty} d\Omega' \frac{\partial \ln \sqrt{G}}{\partial \Omega'}\frac{d\Omega'}{\Omega' - \Omega} \qquad (22)$$

where the upper (lower) sign occurs if $v_{g1} < v_{g2}$ $(v_{g1} > v_{g2})$. It should be pointed out that our analysis assumes a *nonvanishing* group velocity mismatch between signal and idler waves, which enters in (19), and indeed the anomalous dispersive effects we

will discuss later are stronger as the group velocity mismatch term is larger. The most interesting case is that corresponding to $v_{g1} > v_{g2}$ and to a signal wave tuned at a frequency Ω_0 corresponding to a *minimum* of the spectral gain curve $G(\Omega)$, i.e., to a *dip* of the spectral gain. Then, the integral on the right-hand side in (22) is expected to be positive at around $\Omega = \Omega_0$, yielding an abnormal group velocity. A simple QPM grating that realizes a spectral gain curve showing local minima is given, for instance, by the sequence of two $\pm$ square-wave uniform gratings, each of length a and period $\Lambda = 2\pi/\Delta k$, separated by a distance l [see Fig. 11(b)]. This structure closely resembles the two-barrier structure considered in Section II-B, and hence the results found there can be applied, *mutatis mutandis*, to the present case as well. In particular, one has $q(z) = q_0$ for $0 < z < a$, $q(z) = 0$ for $a < z < a+l$, and $q(z) = q_0 \exp(i\Phi)$ for $l+a < z < l+2a$, where $q_0 \equiv (2/\pi)\tilde{d}[8\pi^2 I_3/(\epsilon_0 c_0 n_1 n_2 n_3 \lambda_1 \lambda_2)]^{1/2}$, $\tilde{d}$ is the element of the nonlinear d-tensor of the crystal involved in the parametric interaction, and Φ is a phase term that depends on the phase shift between the two square waves in the two grating sections [see Fig. 11(c)].

The case of major interest is that corresponding to $\Phi = \pi$, for which a gain dip with $G = 1$ is attained at $\Omega_0 = 0$. The corresponding group delay τ_g at $\Omega = 0$, calculated following the analysis of Section II-B, is given by

$$\tau_g = \frac{L}{v_g} - \frac{l}{2}\left(\frac{1}{v_{g2}} - \frac{1}{v_{g1}}\right) \times \left[\cosh^2(q_0 a) + \sinh^2(q_0 a) + \frac{1}{q_0 l}\sinh(2q_0 a)\right]. \quad (23)$$

The condition $G(0) = 1$ means that the amplifier is *transparent* for a signal wave packet tuned at $\Omega = 0$, whereas the transit time of the signal pulse may become superluminal and even negative at sufficiently high pump intensities. From a physical viewpoint, the transparency (i.e., absence of amplification) of the amplifier can be explained as a result of a *cascading process*: in the first QPM grating conversion of the pump wave, leading to amplification of signal and generation of the idler wave, occurs; in the second grating, owing to the phase reversal of d_{eff}, a back conversion process takes place, which makes the amplifier transparent for the signal field. Most important, because of the group velocity mismatch experienced by the copropagating fields, the cascading of the down- and up-conversion processes produces a strong change of the effective group velocity of the signal wave.

To make a quantitative analysis, let us consider a PPLN nonlinear crystal pumped at the wavelength $\lambda_3 = 532$ nm with a signal field at $\lambda_1 = 1.55$ μm ($\lambda_2 = 810$ nm, $\tilde{d} = d_{33} \simeq 27$ pm/V), and assume $a = 3\,\text{mm}$ and $l = 2\,\text{mm}$. From Sellmeir equations [53], one can estimate at 25°C $v_{g1}/c_0 = 0.458\,15$, $v_{g2}/c_0 = 0.442\,20$ and a QPM period $\Lambda \simeq 7.39$ μm, which is easily accessible with current poling technology. Fig. 12 shows the behavior of the group delay τ_g at the dip center of the amplifier as a function of the pump intensity. The effective group velocity becomes superluminal at $I_3 \simeq 105$ MW/cm^2 and negative at $I_3 \simeq 135$ MW/cm^2.

The spectral behavior of power gain G and group delay τ_g versus frequency for $I_3 = 135$ MW/cm^2 is shown in Fig. 13. Notice that, to observe such anomalous values of group delays,

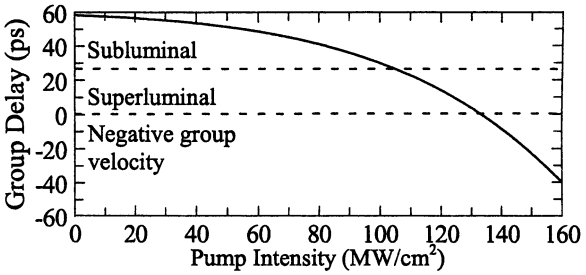

Fig. 12. Behavior of group delay τ_g of the double-grating PPLN amplifier as a function of pump intensity at gain dip. Parameter values are given in the text.

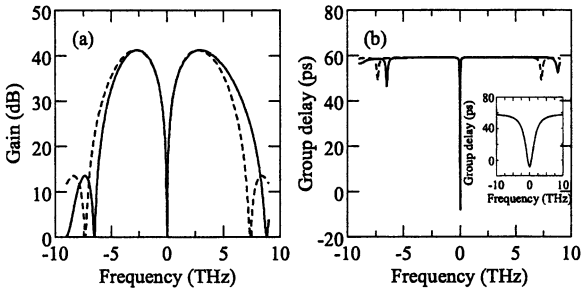

Fig. 13. (a) Spectral power gain G, and (b) corresponding group delay τ_g at signal wavelength, for the PPLN amplifier of Fig. 11(c) and for a pump intensity $I_3 = 135$ MW/cm^2. Solid lines refer to the results obtained by neglecting group velocity due to material dispersion and higher order dispersion effects, as in (17) and (18). Dashed lines are obtained by considering material dispersion at any order using Sellmeier equations. The inset in (b) shows an enlargement of the group delay close to the gain dip.

a parametric gain as high as 40 dB should be reached far from the dip of the gain curve [see Fig. 13(a)]. It is remarkable that the occurrence of superluminal transit times persists when imperfections of the QPM structure from the target case, which are unavoidable in a practical QPM device, are considered. For instance, a deviation of Φ from the ideal value π causes a deformation of the spectral gain curve with a shift of the dip frequency Ω_0 away from zero (see Fig. 14). Despite the large deviations of the spectral gain curve from target 1 [compare, e.g., the inset of Fig. 14 with Fig. 13(a)], the group delay remains superluminal at the dip center for a wide interval around $\Phi = \pi$ (see Fig. 14).

The analytical predictions based on the group delay analysis have been checked by performing direct numerical simulations of pulse propagation in the crystal and assuming a transform-limited Gaussian pulse, tuned at $\Omega = 0$, as a weak probe beam. Fig. 15 shows the traces of incident pulse at $z = 0$ (dotted line) and of transmitted pulses at $z = L$ (solid lines) for increasing values of the pump intensity; we assumed $\Phi = \pi$, an incident pulse duration of 250 ps, and we normalized the pulse intensities to the peak intensity of the incoming pulse. Note that, at the pump intensities corresponding to curves 3 and 4, the transmitted pulse leaves the amplifier *before* the peak of the incident Gaussian pulse has entered into the amplifier. For a quantitative estimation of power and energy levels involved, assuming for instance a Gaussian pump with a beam waist of $\simeq 280$ μm, curve 3 in Fig. 15 corresponds to a pump peak power of $\simeq 170$ kW. Using a pulsed pump of $\sim$5 ns duration (FWHM), i.e., twenty times longer than the probing pulses, a pump pulse energy of $\simeq 0.90$ mJ is required, which can be reached using frequency-doubled Q-switched neodimium-based lasers.

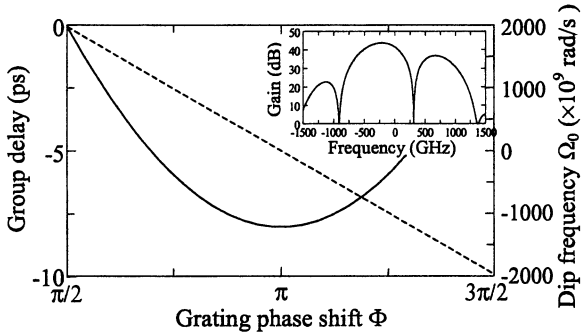

Fig. 14. Behavior of group delay (solid curve) and frequency offset Ω_0 of the principal dip in the spectral gain curve as functions of the phase shift Φ. The inset shows the spectral power gain curve of the amplifier for $\Phi = \pi/2$.

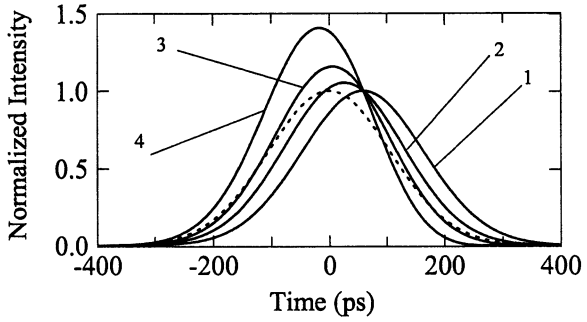

Fig. 15. Intensity pulse traces of a weak signal probe at the exit plane $z = L$, transmitted through the PPLN amplifier, for a few values of the pump intensity. Curve 1, $I_3 = 0$; curve 2, $I_3 = 108$ MW/cm^2; curve 3, $I_3 = 135$ MW/cm^2; curve 4, $I_3 = 162$ MW/cm^2. The dashed curve shows the incident Gaussian probe pulse at the input plane of the amplifier.

V. Conclusion

In this review article, we have provided an overview of recent theoretical and experimental results on anomalous group velocities in optical pulse propagation through linear and nonlinear photonic grating structures. Our analysis has been especially focused on superluminal propagation of picosecond pulses at 1.5 μm in FBGs, and the measurement of tunneling times in the picosecond time scale in different structures has been reported. We also revealed that group velocity control by a pump field is possible exploiting nonlinear interaction processes in nonlinear QPM grating structures.

References

[1] R. Y. Chiao and A. M. Steinberg, "Tunneling times and superluminality," *Prog. Opt.*, vol. XXXVII, pp. 345–405, 1997.

[2] G. Nimtz and W. Heitmann, "Superluminal photonic tunneling and quantum electronics," *Prog. Quantum Electron.*, vol. 21, pp. 81–108, 1997.

[3] W. Heitmann, "Workshop on superluminal velocities," *Ann. Phys. (Leipzig)*, vol. 7, pp. 591–782, 1998.

[4] R. Boyd and D. Gauthier, "Slow and fast light," *Prog. Opt.*, vol. 43, pp. 497–530, 2002.

[5] R. Y. Chiao and P. W. Milonni, "Fast light, slow light," *Opt. Photon. News*, vol. 13, pp. 26–30, 2002.

[6] S. Chu and S. Wong, "Linear pulse propagation in an absorbing medium," *Phys. Rev. Lett.*, vol. 48, pp. 738–741, 1982.

[7] B. Segard and B. Macke, "Observation of negative velocity pulse propagation," *Phys. Lett. A*, vol. 109, pp. 213–216, 1985.

[8] A. M. Steinberg and R. Y. Chiao, "Dispersionless, highly superluminal propagation in a medium with a gain doublet," *Phys. Rev. A*, vol. 49, pp. 2071–2075, 1994.

[9] L. J. Wang, A. Kuzmich, and A. Dogariu, "Gain-assisted superluminal light propagation," *Nature*, vol. 406, pp. 277–279, 2000.

[10] A. Dogariu, A. Kuzmich, and L. J. Wang, "Transparent anomalous dispersion and superluminal light-pulse propagation at a negative group velocity," *Phys. Rev. A*, vol. 63, pp. 053 806 1–12, 2001.

[11] G. S. Agarwal, T. N. Dey, and S. Menon, "Knob for changing light propagation from subluminal to superluminal," *Phys. Rev. A*, vol. 60, pp. 053 809 1–4, 2001.

[12] A. Enders and G. Nimtz, "Photonic-tunneling experiments," *Phys. Rev. B*, vol. 47, pp. 9605–9609, 1993.

[13] A. Ranfagni, P. Fabeni, G. P. Pazzi, and D. Mugnai, "Anomalous pulse delay in microwave propagation: A plausible connection to the tunneling time," *Phys. Rev. E*, vol. 48, pp. 1453–1460, 1993.

[14] A. M. Steinberg, P. G. Kwiat, and R. Y. Chiao, "Measurement of the single-photon tunneling time," *Phys. Rev. Lett.*, vol. 71, pp. 708–711, 1993.

[15] G. Nimtz, A. Enders, and H. Spieker, "Photonic tunneling times," *J. Phys. I (France)*, vol. 4, pp. 565–570, 1994.

[16] C. Spielmann, R. Szipocs, A. Stingl, and F. Krausz, "Tunneling of optical pulses through photonic band gaps," *Phys. Rev. Lett.*, vol. 73, pp. 2308–2311, 1994.

[17] P. Balcou and L. Dutriaux, "Dual optical tunneling times in frustrated total internal reflection," *Phys. Rev. Lett.*, vol. 78, pp. 851–854, 1997.

[18] M. Scalora, R. J. Flynn, S. B. Reinhardt, R. L. Fork, M. J. Bloemer, M. D. Tocci, C. M. Bowden, H. S. Ledbetter, J. M. Bendickson, J. P. Dowling, and R. P. Leavitt, "Ultrashort pulse propagation at the photonic band edge: Large tunable group delay with minimal distortion and loss," *Phys. Rev. E*, vol. 54, pp. R1078–R1081, 1996.

[19] J. Khurgin, "Light slowing down in moire fiber gratings and its implications for nonlinear optics," *Phys. Rev. A*, vol. 62, pp. 013 820 1–4, 2000.

[20] V. N. Astratov, R. M. Stevenson, I. S. Culshaw, D. M. Whittaker, M. S. Skolnick, T. F. Krauss, and R. M. De La Rue, "Heavy photon dispersions in photonic crystal waveguides," *Appl. Phys. Lett.*, vol. 77, pp. 178–180, 2000.

[21] G. Lenz, B. J. Eggleton, C. K. Madsen, and R. E. Slusher, "Optical delay lines based on optical filters," *IEEE J. Quantum Electron.*, vol. 37, pp. 525–532, Apr. 2001.

[22] S. Longhi, "Superluminal pulse reflection in asymmetric one-dimensional photonic band gaps," *Phys. Rev. E*, vol. 64, pp. 037 601 1–4, 2001.

[23] S. Longhi, M. Marano, P. Laporta, and M. Belmonte, "Superluminal optical pulse propagation at 1.5 μm wavelength in periodic fiber Bragg gratings," *Phys. Rev. E*, vol. 64, pp. 055 602(R) 1–4, 2001.

[24] S. Longhi, M. Marano, P. Laporta, O. Svelto, and M. Belmonte, "Propagation, manipulation, and control of picosecond optical pulses at 1.5 μm in fiber Bragg gratings," *J. Opt. Soc. Amer. B*, vol. 12, pp. 2742–2757, 2002, to be published.

[25] S. Longhi, P. Laporta, M. Belmonte, and E. Recami, "Measurement of superluminal optical tunneling times in double-barrier photonic band gaps," *Phys. Rev. E*, vol. 65, pp. 046 610 1–6, 2002.

[26] S. Longhi, M. Marano, P. Laporta, M. Belmonte, and P. Crespi, "Experimental observation of superluminal pulse reflection in a double-Lorentzian photonic band gap," *Phys. Rev. E*, vol. 65, pp. 045 602(R) 1–4, 2002.

[27] S. Longhi, M. Marano, and P. Laporta, "Dispersive properties of quasiphase-matched optical parametric amplifiers," *Phys. Rev. A*, vol. 66, pp. 033803–1–033803–10, 2002, to be published.

[28] S. Longhi, "Negative group velocities in cascading $\chi^{(2)}$ nonlinear optical interactions," *Europhys. Lett.*, vol. 60, pp. 214–219, 2002, to be published.

[29] T. E. Hartman, "Tunneling of a wave packet," *J. Appl. Phys.*, vol. 33, pp. 3427–3434, 1962.

[30] V. S. Olkhovsky, E. Recami, and G. Salesi, "Superluminal tunneling through two successive barriers," *Europhys. Lett.*, vol. 57, pp. 879–884, 2002.

[31] P. Yeh, *Optical Waves in Layered Media*. New York: Wiley, 1988.

[32] L. Poladian, "Resonance mode expansions and exact solutions for nonuniform gratings," *Phys. Rev. E*, vol. 54, pp. 2963–2975, 1996.

[33] V. S. Olkhovsky and E. Recami, "Recent developments in the time analysis of tunnelling processes," *Phys. Rep.*, vol. 214, pp. 339–356, 1992.

[34] A. P. L. Barbero, H. E. Hernandez-Figueroa, and E. Recami, "Propagation speed of evanescent modes," *Phys. Rev. E*, vol. 62, pp. 8628–8635, 2000.

[35] M. Mojahedi, E. Schamiloglu, F. Hegeler, and K. J. Malloy, "Time-domain detection of superluminal group velocity for single microwave pulses," *Phys. Rev. E*, vol. 62, pp. 5758–5766, 2000.

[36] J. D. Jackson, *Classical Electrodynamics*. New York: Wiley, 1975.

[37] P. Laporta, S. Taccheo, S. Longhi, O. Svelto, and C. Svelto, "Erbium-yt-terbium microlasers: optical properties and lasing characteristics," *Opt. Materials*, vol. 11, pp. 269–288, 1999.
[38] B. Costa, M. Puleo, and E. Vezzoni, "Phase-shift technique for the measurement of chromatic dispersion in single-mode optical fibers using LEDs," *Electron. Lett.*, vol. 19, pp. 1074–1076, 1983.
[39] S. Ryu, Y. Horiuchi, and K. Mochizuky, "Novel chromatic dispersion measurement method over continuous gigahertz tuning range," *J. Lightwave Technol.*, vol. 7, pp. 1177–1180, Aug. 1989.
[40] H. M. Brodowsky, W. Heitmann, and G. Nimtz, "Comparison of experimental microwave tunneling data with calculations based on Maxwell's equations," *Phys. Lett. A*, vol. 222, pp. 125–129, 1996.
[41] G. Nimtz and A. Enders, "On superluminal barrier traversal," *J. Phys. I (France)*, vol. 2, pp. 1693–1698, 1992.
[42] E. Merzbacher, *Quantum Mechanics*. New York: Wiley, 1970, ch. 6 and 7.
[43] P. Pereyra, "Closed formulas for tunneling time in superlattices," *Phys. Rev. Lett.*, vol. 84, pp. 1772–1775, 2000.
[44] T. Tsai and G. Thomas, "Analog between optical waveguide system and quantum-mechanical tunneling," *Amer. J. Phys.*, vol. 44, pp. 636–638, 1976.
[45] T. Erdogan, "Fiber grating spectra," *J. Lightwave Technol.*, vol. 15, pp. 1277–1294, Aug. 1997.
[46] L. Poladian, "Group-delay reconstruction for fiber Bragg gratings in reflection and transmission," *Opt. Lett.*, vol. 22, pp. 1571–1573, 1997.
[47] G. H. Song and S. Y. Shin, "Design of corrugated waveguide filters by the Gel'fand-Levitan-Marchenko inverse-scattering methods," *J. Opt. Soc. Amer. A*, vol. 2, pp. 1905–1915, 1985.
[48] M. M. Fejer, *Beam Shaping and Control With Nonlinear Optics*, F. Kajzar and R. Reinisch, Eds. New York: Plenum, 1998, p. 375.
[49] G. Imeshev, A. Galvanauskas, D. Harter, M. A. Arbore, M. Proctor, and M. M. Fejer, "Engineerable femtosecond pulse shaping by second-harmonic generation with fourier synthetic quasiphase-matching gratings," *Opt. Lett.*, vol. 23, pp. 864–866, 1998.
[50] G. Imeshev, M. A. Arbore, M. M. Fejer, A. Galvanauskas, M. Fermann, and D. Harter, "Ultrashort-pulse second-harmonic generation with longitudinally nonuniform quasiphase-matching gratings: Pulse compression and shaping," *J. Opt. Soc. Amer. B*, vol. 17, pp. 304–318, 2000.
[51] G. Imeshev, M. M. Fejer, A. Galvanauskas, and D. Harter, "Pulse shaping by difference-frequency mixing with quasiphase-matching gratings," *J. Opt. Soc. Amer. B*, vol. 18, pp. 534–539, 2001.
[52] M. Blaauboer, A. G. Kofman, A. E. Kozhekin, G. Kurizki, D. Lenstra, and A. Lodder, "Superluminal optical phase conjugation: pulse shaping and instability," *Phys. Rev. A*, vol. 57, pp. 4905–4912, 1998.
[53] G. J. Edwards and M. Lawrence, "A temperature-dependent dispersion equation for congruently grown lithium niobate," *Opt. Quantum Electron.*, vol. 16, pp. 373–375, 1984.
[54] G. Kurizki, A. Kozhekin, and A. G. Kofman, "Tachyons and information transfer in quantized parametric amplifiers," *Europhys. Lett.*, vol. 42, pp. 499–504, 1998.

Stefano Longhi was born in Bergamo, Italy, in 1967. He received the M.S. degree in electronic engineering (*cum laude*) and the Ph.D. degree in physics from the Polytechnic Institute of Milan, Italy, in 1992 and 1995, respectively.

He has held a postdoctoral research position with INFM and CNR, Milan and has served a one-year postdoctoral position at MIT, Cambridge, MA. Since 1998 he has been an Assistant Professor of General Physics and Quantum Electronics at the Physics Department, Polytechnic Institute of Milan. His research covers a wide range of both experimental and theoretical activities in the fields of laser physics, nonlinear optics and quantum electronics. These include development of near-infrared solid-state lasers, ultrashort-pulse generation and manipulation for optical communications, nonlinear dynamics and solitons in optical systems, and optical pattern formation.

Dr. Longhi has authored and coauthored more than 80 scientific papers in peer-referred international journals.

Marcello Marano was born in Milan, Italy, in 1974. He received the M.S. degree in telecommunications engineering (*cum laude*) from the Polytechnic Institute of Milan in 1999. He is pursuing the Ph.D. degree in electronics and communications engineering at the Polytechnic Institute of Milan.

In 2001, he joined the Physics Department of the Polytechnic Institute of Milan as an Assistant Professor of Physics. His current research activities are in the fields of development of solid-state lasers for applications to optical communications, generation and manipulation of ultrahigh repetition-rate pulse trains, frequency and amplitude stabilization of solid-state lasers for metrology and atmosphere monitoring.

Michele Belmonte was born in Milan, Italy, in 1971. He received the M.S. degree in nuclear engineering from the Polytechnic Institute of Milan.

From 1999 to 2001, he was a researcher with Pirelli Componenti Ottici, Milan, Italy and was responsible for the design and fabrication of fiber Bragg gratings. Since 2001 he has been with Corning OTI, Milan. His current research areas are in the fields of fiber Bragg grating modeling and fabrication, lithium niobate amplitude modulators for high-speed signal generation, and frequency conversion in lithium niobate waveguide devices.

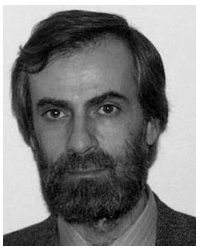

Paolo Laporta is a Professor of Optics with the Physics Department of the Polytechnic Institute of Milan, Italy. His research activities include laser applications to biology and biomedicine, ultrashort light pulse generation, advanced laser resonator for solid-state lasers, diode-pumped solid-state lasers, erbium lasers and amplifiers for optical communications, frequency and amplitude stabilization of solid-state lasers for metrology, photonic waveguide devices, and photonic crystals.

Prof. Laporta is the author of more than 100 scientific papers and his research has been the subject of 21 invited papers at international conferences. He has served as Topical Session Chair at the CLEO-Europe conference 2000 and as Program Co-chair at the Progress in Solid-State Lasers Conference, Munich, 2001. In 1992, he received the Philip Morris Prize for Science and Technology.